Proceeding of the 11th World Congress on Intelligent Control and Automation
Shenyang, China, June 29 - July 4 2014

A Weighted Damping Coefficient Based Manipulability Maximizing Scheme for Coordinated Motion Planning of Wheeled Mobile Manipulators*

Yunong Zhang, Xiaogang Yan, Weibing Li, Dongsheng Guo and Jun Li
School of Information Science and Technology, Sun Yat-sen University, Guangzhou 510006, P. R. China
SYSU-CMU Shunde International Joint Research Institute, Shunde 528300, P. R. China
zhynong@mail.sysu.edu.cn; jallonzyn@sina.com

Abstract— **A novel weighted damping coefficient based manipulability maximizing (WDCMM) scheme is proposed and investigated in this paper for the motion planning of wheeled mobile redundant manipulators. Such a scheme treats the mobile platform and the redundant manipulator as a whole system, and is thus called a coordinated control scheme. In order to improve the manipulability during the end-effector task execution, a manipulability maximizing index is firstly incorporated into the scheme formulation. To remedy the manipulator's manipulability decreasing and/or the joint variables' abrupt change (MDJVAC) problem, a weighted damping coefficient matrix is further introduced and considered in such a scheme. For verifying the performance of the proposed WDCMM scheme, we analyze a mobile manipulator model composed of a wheeled mobile platform and a six degrees-of-freedom (DOF) manipulator. Simulations performed on the wheeled mobile manipulator model substantiate well the effectiveness, accuracy and superiority of the proposed WDCMM scheme.**

Index Terms— **Wheeled mobile manipulators; coordinated motion planning; manipulability maximizing; weighted damping coefficient; redundancy resolution.**

I. Introduction

A manipulator is called redundant when it possesses more degrees-of-freedom (DOF) than required to execute a user-specified primary end-effector task [1], [2]. A lot of research efforts have been devoted to the investigation of various fixed-base redundant manipulators. In recent years, research interests have been increasingly given to mobile manipulators due to their combination of mobility and dexterity [2]. In general, finding the optimal solution to the robotic kinematics by designing various performance indices is the basic research methodology. The manipulators' kinematic manipulability index is one of such indices [3], which is proposed for solving the so-called singularity problem arising in the motion control of redundant manipulators.

As proved in [4], kinematic singularities can not be avoided in the simple pseudoinverse approach, since it may generate trajectories which pass arbitrarily close to singular points in joint space. Such a situation could occur in mobile manipulators with higher possibility than in fixed-base manipulators. This would result in the manipulator's manipulability decreasing and/or the joint variables' abrupt change (MDJVAC) problem during the end-effector task execution, even if a traditional pseudoinverse-based manipulability maximizing scheme is used.

To solve such an MDJVAC problem, this paper exploits a damping technique in the motion planning of mobile manipulators. Since the redundancy resolution of a mobile manipulator is usually considered as an optimal control problem [5], a properly designed coordinated scheme (e.g., the proposed motion planning scheme) can naturally lead to the optimization of the whole system. That is, the proposed coordinated motion planning scheme is closely related to the optimal control of the whole robotic system that aims at exploiting the mobility of the platform and achieving the optimal manipulability of the mobile manipulator.

II. Kinematic Modeling of WMSDM

In this section, the kinematic modeling of the wheeled mobile six-DOF manipulator (WMSDM) is given. The computer-aided design (CAD) model of such an WMSDM system is shown in Fig. 1. As seen from the figure, the WMSDM system is composed of a six-DOF spatial manipulator and a mobile platform with two independently driving wheels (and two passive omni-directional supporting wheels). According to [6], the integrated kinematics of the WMSDM at the velocity level is obtained in the following form:

$$\dot{r}_{\mathrm{w}} = J(\vartheta)\dot{q}, \tag{1}$$

where $\dot{r}_{\mathrm{w}} \in R^m$ is the time derivative of the manipulator's end-effector position/orientation vector r_{w} in Cartesian space with respect to the world coordinate frame. In addition, $J(\vartheta) \in R^{m\times(2+n)}$ is the Jacobian matrix, with vector $\vartheta = [\phi, \theta^{\mathrm{T}}]^{\mathrm{T}} \in R^{1+n}$ and superscript $^{\mathrm{T}}$ denoting the transpose operator. Besides, ϕ is the orientation angle of the mobile platform, and $\theta \in R^n$ denotes the joint-angle vector of the six-DOF manipulator. Note that, by defining $\varphi \in R^2$ as the driving wheel angle (angular position) vector, we have the combined angle vector $q = [\varphi^{\mathrm{T}}, \theta^{\mathrm{T}}]^{\mathrm{T}} \in R^{2+n}$, and its time derivative $\dot{q} = [\dot{\varphi}^{\mathrm{T}}, \dot{\theta}^{\mathrm{T}}]^{\mathrm{T}}$ (i.e., the combined velocity vector).

*This work is supported by the National Natural Science Foundation of China (under grants 61075121 and 60935001), the Specialized Research Fund for the Doctoral Program of Institutions of Higher Education of China (with project number 20100171110045), and the Guangdong Provincial Innovation Training Program for University Students (with project number 1055813063). Kindly note that all authors of the paper are jointly of the first authorship.

978-1-4799-5825-2/14/$31.00 ©2014 IEEE

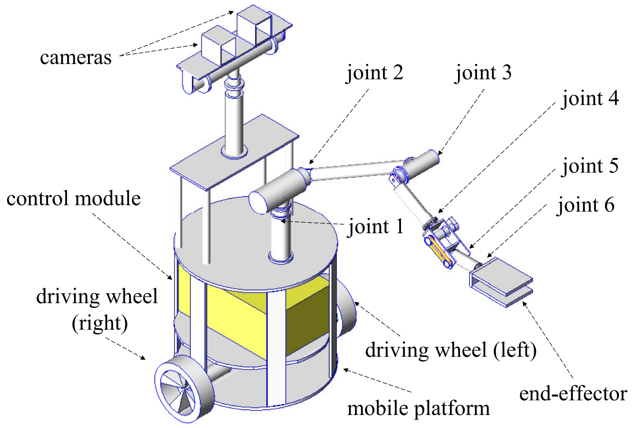

Fig. 1. The CAD model of the WMSDM system.

III. Problem and Scheme Descriptions

In this section, the weighted damping coefficient based manipulability maximizing (WDCMM) scheme is proposed and investigated for the presented wheeled mobile manipulator. Specifically, a traditional pseudoinverse-based redundancy-resolution scheme aimed at minimizing the WMSDM manipulability is firstly presented, which may result in the MDJVAC problem. Based on the analysis about the MDJVAC problem, the solution by adopting the damping technique is thus developed, which is termed the WDCMM scheme in this paper for the wheeled mobile manipulator.

A. Scheme with MDJVAC Problem

In the previous section, the velocity-level kinematics of the mobile manipulator has been obtained as $\dot{r}_{\mathrm{w}} = J(\vartheta)\dot{q}$, i.e., (1). For solving the motion planning problem, i.e., to generate $\dot{q}$ with desired path $\dot{r}_{\mathrm{dw}}$ given, a general pseudoinverse-based scheme is formulated as follows [2]:

$$\dot{q} = \dot{q}_{\mathrm{p}} + \dot{q}_{\mathrm{h}} = J^{\dagger}\dot{r}_{\mathrm{dw}} + \nu\left(I - J^{\dagger}J\right)\xi, \tag{2}$$

where $J^{\dagger} \in R^{(2+n)\times m}$ denotes the pseudoinverse of the Jacobian matrix J, $\dot{r}_{\mathrm{dw}} \in R^{m}$ denotes the time-derivative of the desired Cartesian path r_{dw}, $I \in R^{(2+n)\times(2+n)}$ denotes the identity matrix, $\nu \in R$ is a constant coefficient and $\xi \in R^{2+n}$ could be an arbitrary vector usually selected by different optimization criteria. Besides, $\dot{q}_{\mathrm{p}} = J^{\dagger}\dot{r}_{\mathrm{w}}$ denotes the particular solution (i.e., the minimum Euclidean-norm solution) to $\dot{r}_{\mathrm{w}} = J\dot{q}$; and $\dot{q}_{\mathrm{h}} = \nu(I - J^{\dagger}J)\xi$ denotes the homogeneous solution corresponding to the manipulator's self-motion, without affecting the end-effector motion but with nonzero initial velocity possibly occurring. Therefore, we can choose different values of coefficient ν to make the solution to be more approximate to the particular solution or the homogeneous solution, and the dilemma about how to choose a suitable value of coefficient ν is discussed below.

Furthermore, in the manipulability maximizing motion planning scheme, the vector ξ can be chosen as the gradient of the manipulability measure w; i.e., let $\xi = \partial w/\partial q$. In this paper, with $\det(\cdot)$ denoting the determinant of a matrix, $w = \det(JJ^{\mathrm{T}})$ is the quantitative measure of the manipulability at the configuration ϑ. By choosing ξ as the above-mentioned gradient of w and set $\nu > 0$ (with the maximum purpose), the manipulator's manipulability can thus be maximized and then the manipulator can be kept away from singularities, while conducting the end-effector task.

However, how to choose a suitable value of coefficient ν could be in the following dilemma.

1) If coefficient ν is set too small, (2) would reduce approximately to $\dot{q} = \dot{q}_{\mathrm{p}} = J^{\dagger}\dot{r}_{\mathrm{w}}$, which is the so-called minimum-velocity-norm (MVN) scheme. Kinematic singularities can not be avoided in the MVN solution, by which the trajectories generated could pass arbitrarily close to singular points in the joint space. For wheeled mobile manipulators, such a singularity problem occurs more frequently since tasks of constructing or drawing on large-scale objects are usually assigned to them.
2) If coefficient ν is set too large, the gradient of the manipulability index will be magnified inappropriately. As a result, the resolved $\dot{q}$ may be of undesirable big magnitude, or even abrupt change of $\dot{q}$ could arise, when the mobile manipulator is near singularities. Thus, coefficient ν should not be set too large.

B. WDCMM Scheme

For solving the MDJVAC problem arising in the traditional pseudoinverse-based scheme (2), the WDCMM scheme is proposed in this subsection. Specifically, if the mobility of the platform can be improved, or $\dot{\theta}$ is restricted (e.g., damped) appropriately, the resolved $\dot{\theta}$ will stop stretching the manipulator towards a singular state before the six-DOF manipulator's Jacobian matrix gets nearly singular. For damping or minimizing $\dot{\theta}$ (or $\|\dot{\theta}\|_2$) slightly, and incorporating it effectively into the redundancy resolution scheme, the combined velocity vector $\dot{q}$ is damped by expanding the task space as follows:

$$\begin{bmatrix} \dot{r}_{\mathrm{w}} \\ \mathbf{0} \end{bmatrix} = \begin{bmatrix} J \\ \eta\Lambda \end{bmatrix} \dot{q}, \tag{3}$$

where $\mathbf{0} \in R^{2+n}$ is a null vector, and $\Lambda \in R^{(2+n)\times(2+n)}$ is the weighted damping matrix. By defining Λ properly, the contribution of $\dot{\varphi}$ and $\dot{\theta}$ to the end-effector velocity can be scaled. In this paper, $\Lambda = \mathrm{diag}(0, 0, 1, 1, 1, 1, 1, 1)$ is a diagonal matrix. Besides, $\eta > 0 \in R$ is a constant coefficient used to scale the magnitude of the manipulator response to the weighted damping matrix Λ. Note that a large value of η motivates the mobility of the platform, but it would increase the positioning error of the mobile manipulator. Thus, η should be chosen experimentally to achieve a balanced performance.

Moreover, due to the existence of the computational round-off error and modeling error, the closed-loop control is necessary. Therefore, to achieve higher precision of the end-effector positioning, the feedback of position error $\lambda_{\mathrm{p}}(r_{\mathrm{dw}} - g(p))$ can be elegantly introduced, where the feedback-gain coefficient $\lambda_{\mathrm{p}} > 0$ (e.g., 20) is used to scale the magnitude of the

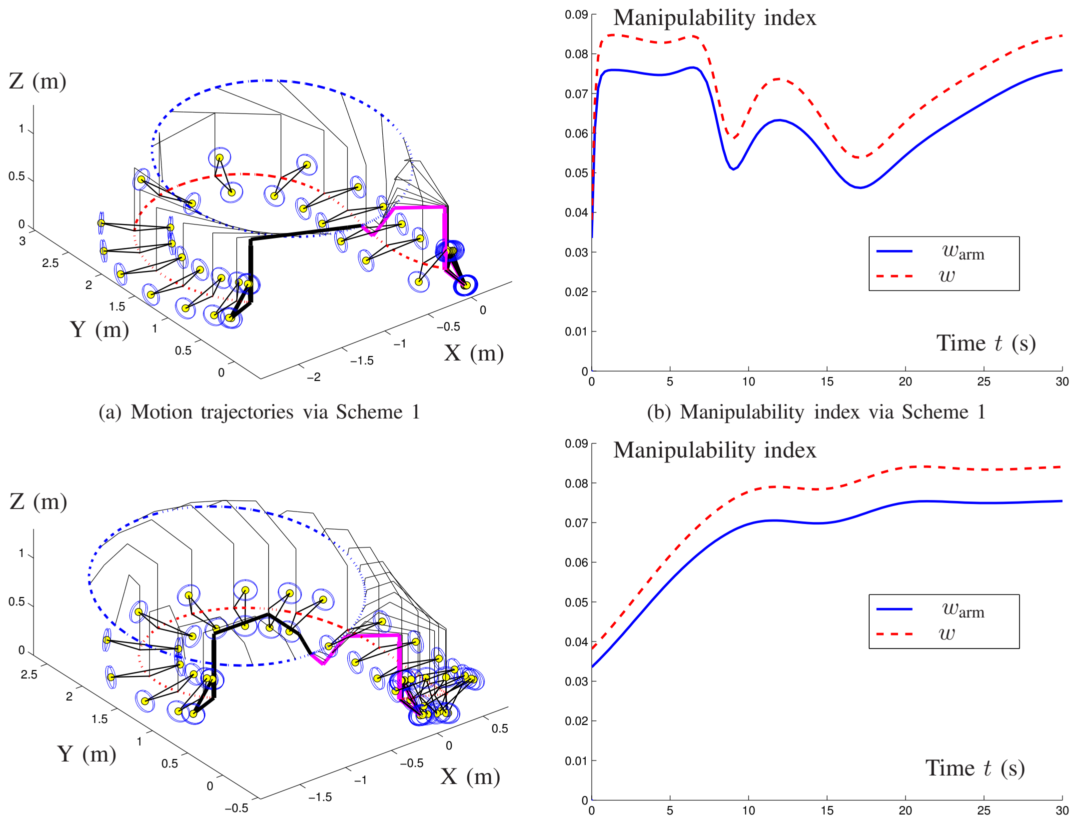

(a) Motion trajectories via Scheme 1
(b) Manipulability index via Scheme 1
(c) Motion trajectories via proposed Scheme 2
(d) Manipulability index via proposed Scheme 2

Fig. 2. Comparison on motion and manipulability when the WMSDM end-effector tracks a circular path, as synthesized by schemes shown in Table I.

TABLE I
COEFFICIENT SETTINGS OF DIFFERENT SCHEMES IN THE SIMULATIONS

Coefficient	Scheme 1	Scheme 2 (WDCMM scheme)
ν	6	6
η	0	0.01

manipulator response to the position error $(r_{\text{dw}} - g(p))$. In addition, $p = [x_G, y_G, \vartheta^{\text{T}}]^{\text{T}} \in R^{3+n}$ is the wheeled mobile manipulator's state vector, where G denotes the six-DOF manipulator's base location, and its position vector with respect to the world coordinate frame $\{\text{w}\}$ is $[x_G, y_G, z_G]^{\text{T}}$ (note that $z_G = 0$ for modeling convenience), together with the velocity vector of point G in $\{\text{w}\}$ being $[\dot{x}_G, \dot{y}_G, \dot{z}_G]^{\text{T}}$. Besides, throughout the paper, the initial coordinate $(x_G(0), y_G(0))$ of G is $(0, 0)$ m. Note that $g(\cdot)$ is a nonlinear mapping from R^{3+n} to R^m, and that $r_{\text{w}} = g(p)$ is the kinematics of the mobile manipulator at the position level.

Thus, based on the above analysis as well as (3), the WDCMM scheme for wheeled mobile manipulators is

$$\dot{q} = \begin{bmatrix} J \\ \eta\Lambda \end{bmatrix}^{\dagger} \begin{bmatrix} \dot{r}_{\text{dw}} + \lambda_{\text{p}}(r_{\text{dw}} - g(p)) \\ \mathbf{0} \end{bmatrix} + \nu(I - J^{\dagger}J)\xi. \quad (4)$$

With $i = 1, 2, \cdots, (2+n)$, the ith element of ξ can be given mathematically as

$$\xi_i = \frac{\partial \det(JJ^{\text{T}})}{\partial q_i} = \det(JJ^{\text{T}}) \operatorname{tr}\left((JJ^{\text{T}})^{-1}\frac{\partial(JJ^{\text{T}})}{\partial q_i}\right)$$
$$= \det(JJ^{\text{T}}) \operatorname{tr}\left((JJ^{\text{T}})^{-1}\left(\frac{\partial J}{\partial q_i}J^{\text{T}} + J\left(\frac{\partial J}{\partial q_i}\right)^{\text{T}}\right)\right),$$

where $\text{tr}(\cdot)$ denotes the trace of a matrix. By properly choosing η and ν, the redundancy-resolution scheme (4) can maximize the mobile manipulator system's manipulability, in addition to fulfilling the given end-effector task, without causing abrupt-change and big-magnitude problems of the resolved $\dot{q}$. The efficacy of such a scheme is illustrated and demonstrated in the ensuing section.

IV. SIMULATIVE VERIFICATION

In this section, computer simulations are performed on the WMSDM with two path-tracking examples (i.e., a circular path and a V-shaped path) given. It is worth pointing out that the circular path and V-shaped path represent straight-line type paths and curve type paths, respectively.

- In the first example, the desired motion of the mobile manipulator's end-effector is a circular path, with the radius being 1.2 m, with the dihedral angle between the path plane and the XY plane being $\pi/24$ rad, and with the task duration being $D = 30$ s. The manipulator's

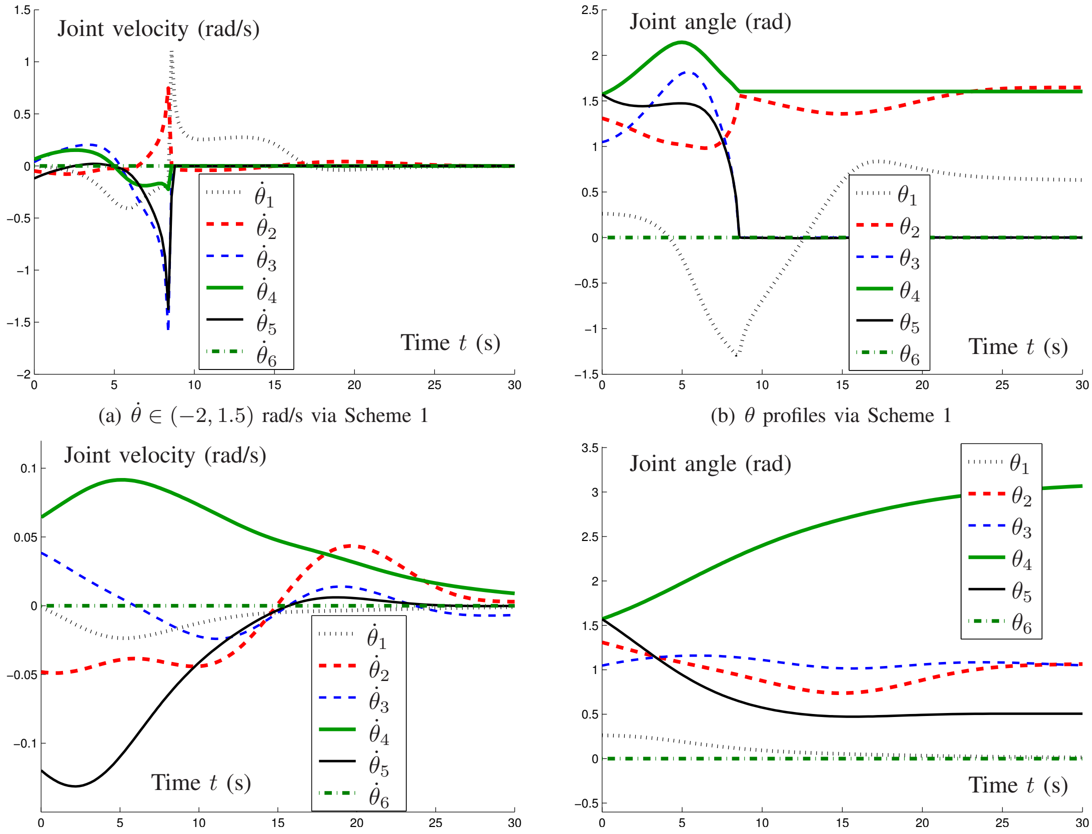

(a) $\dot{\theta} \in (-2, 1.5)$ rad/s via Scheme 1

(b) θ profiles via Scheme 1

(c) $\dot{\theta} \in (-0.2, 0.1)$ rad/s via proposed Scheme 2

(d) θ profiles via proposed Scheme 2

Fig. 3. Comparison on joint-angle θ and joint-velocity $\dot{\theta}$ profiles when the WMSDM end-effector tracks the circular path, as synthesized by the schemes.

initial joint state $\theta(0) = [\pi/12, 5\pi/12, \pi/3, \pi/2, \pi/2, 0]^{\mathrm{T}}$ rad, and the initial orientation angle $\phi(0)$ of the wheeled mobile platform is $7\pi/8$ rad.

- In the second example, the manipulator's end-effector is expected to track a V-shaped path, where each line segment length is 3.5 m, the path plane is parallel to the XY plane, and the task duration $D = 20$ s. The manipulator's initial joint state $\theta(0) = [\pi/6, \pi/2, \pi/3, -\pi/2, -\pi/2, 0]^{\mathrm{T}}$ rad, and the initial orientation angle $\phi(0)$ of the wheeled mobile platform is $\pi/3$ rad.

A. *Circular-Path Tracking Example*

In order to demonstrate the efficacy and superiority of the proposed WDCMM scheme, two schemes (termed Scheme 1 and Scheme 2) are generated by setting different values of coefficients ν and η in (4), as shown in Table I. In this circular-path tracking example, the redundancy resolution problem of the WMSDM is solved by Schemes 1 and 2, respectively. Note that, with $\eta = 0$, the WDCMM scheme becomes a general pseudoinverse-based method considering manipulability maximization. The corresponding comparative simulation results of tracking the circular path are shown in Figs. 2–4, which are synthesized by Schemes 1 and 2.

Firstly, Fig. 2 shows the trajectories of motion and manipulability measure of the simulated mobile manipulator, of which the end-effector tracks the path, as synthesized by Schemes 1 and 2. Specifically, Fig. 2(a) and (b) shows the simulation results synthesized by Scheme 1. As seen from Fig. 2(a), during the end-effector task execution, Links 2–6 are in a straight line in most of the time. That is to say, by using a small value of coefficient $\nu = 6$ but without adopting the damping technique (i.e., by setting $\eta = 0$), the manipulator is still at a singular configuration. In addition, both of the manipulability measure of the manipulator (simply put, arm) and that of the whole system [i.e., $w_{\text{arm}} = \det(J_{\text{arm}} J_{\text{arm}}^{\mathrm{T}})$ and $w = \det(JJ^{\mathrm{T}})$, respectively] are of low values as shown in Fig. 2(b). It is worth pointing out that, even when w_{arm} is (nearly) zero, w can still be nonzero (though it is quite small). Thus, the mobile platform increases the capability of such a system. Similarly, Fig. 2(c) and (d) shows the simulation results synthesized by Scheme 2. As seen from these two subfigures, the configuration of the WMSDM is well improved during the end-effector task execution, and the end-effector task is completed well. That is to say, the manipulability of the mobile-manipulator system can be improved well by using a small value of coefficient ν but adopting the damping technique, i.e., by setting $\eta = 0.01$.

Secondly, the joint-variable profiles are shown in Fig. 3. From Fig. 3(a), which shows the simulated joint-velocity profiles, it can be seen that saltus occurs at around $t = 8$ s by using Scheme 1. Such abrupt phenomena in the $\dot{\theta}$ solution

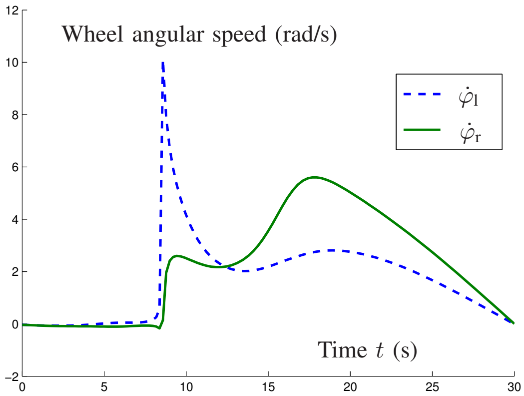

(a) $\dot{\varphi} \in (-2, 12)$ rad/s via Scheme 1

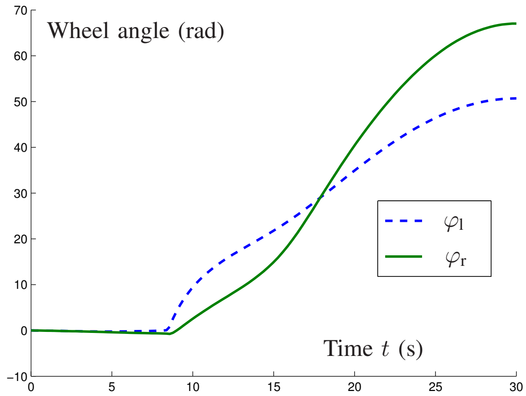

(b) φ profiles via Scheme 1

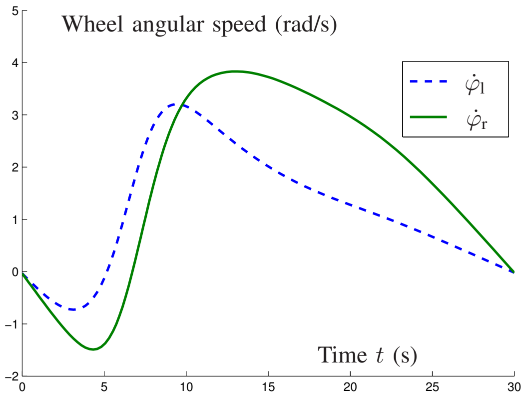

(c) $\dot{\varphi} \in (-2, 5)$ rad/s via proposed Scheme 2

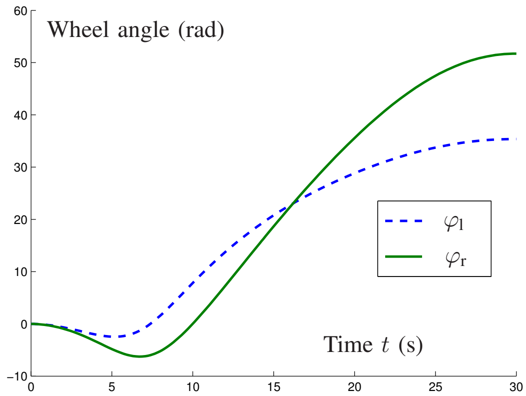

(d) φ profiles via proposed Scheme 2

Fig. 4. Comparison on φ and $\dot{\varphi}$ profiles when the WMSDM end-effector tracks the circular path, as synthesized by the schemes.

are undesirable for engineering application. By contrast, as seen from Fig. 3(c), all joint-velocities vary continuously and smoothly during the task execution. Moreover, from Fig. 3(a) and (c), we can observe that the maximum value of joint velocities synthesized by Scheme 2 is less than 0.2 rad/s, which is much smaller than those synthesized by Scheme 1 (i.e., over 1.5 rad/s). It is worth pointing out that, due to the different ranges of joint velocities synthesized by Schemes 1 and 2, we choose different scales of the coordinate systems in Fig. 3(a) and (c) for better presentation and understanding. Therefore, the performance of proposed Scheme 2 is superior. Corresponding joint-angle profiles shown in Fig. 3(b) and (d) also demonstrate that, by adopting the WDCMM scheme with $\nu = 6$ and $\eta = 0.01$, the resultant θ profiles are smoother than those synthesized by Scheme 1.

Thirdly, Fig. 4 shows the profiles of driving wheels' angle φ and angular speed $\dot{\varphi}$, where subscripts $_l$ and $_r$ correspond to the left and right driving wheels, respectively. From the figure, we see clearly the superior performance of Scheme 2, because the profiles of driving wheel angular speed and angle synthesized by Scheme 2 are much smoother than those by Scheme 1. In addition, the corresponding positioning error synthesized by Scheme 2 is tiny, with its maximum value less than 2.5×10^{-6} m. This demonstrates well the high accuracy of the proposed WDCMM scheme (i.e., Scheme 2).

Thus, based on the above simulation results, it can be summarized that the proposed WDCMM scheme [i.e., (4) with $\nu = 6$ and $\eta = 0.01$] is a good alternative for the optimal motion planning of wheeled mobile manipulators, in view of its superior performance in manipulability maximization of mobile manipulators and suitability for practical applications.

B. V-Shaped Path Tracking Example

As the second example, simulations of V-shaped path tracking are performed comparatively and further to substantiate the efficacy of the proposed WDCMM scheme.

Synthesized by the proposed WDCMM scheme, the simulation results are illustrated in Fig. 5. Specifically, Fig. 5(a) shows the motion trajectories of the mobile manipulator. From the subfigure, it can be seen that the WMSDM end-effector path tracking task is fulfilled well. In addition, the joint configuration is adjusted and kept away from singular configurations. The resolved joint velocity $\dot{\theta}$ is illustrated in Fig. 5(b), showing that the resolved variables are all continuous and smooth throughout the end-effector task execution. Moreover, Fig. 5(c) shows the corresponding positioning error ϵ, with its maximum value less than 2.5×10^{-5} m. As seen from Fig. 5(c), the maximum positioning error occurs when the end-effector moves to the turning point of the V-shaped path at around $t = 10$ s. Besides, Fig. 5(d) illustrates the profiles of the manipulability

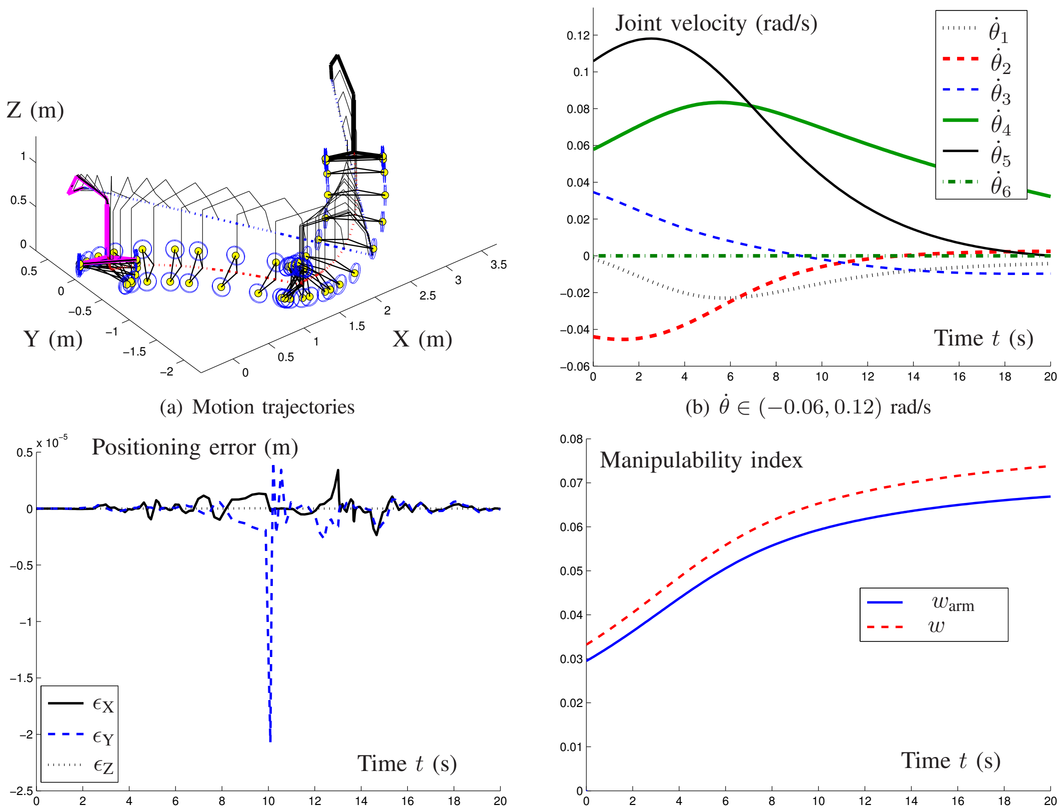

(a) Motion trajectories

(b) $\dot{\theta} \in (-0.06, 0.12)$ rad/s

(c) Positioning error $\epsilon \in (-2.5 \times 10^{-5}, 0.5 \times 10^{-5})$ m

(d) Manipulability index

Fig. 5. Simulation results of the WMSDM end-effector tracking the V-shaped path synthesized by the proposed WDCMM scheme with $\nu = 6$ and $\eta = 0.01$.

measures of the six-DOF manipulator and the whole system, which are increasing throughout the task duration. That is, with the manipulability maximizing index considered and by exploiting the damping technique, the manipulability of the WMSDM can be increased effectively, and the end-effector task is completed as well. These simulation results demonstrate again the efficacy and high accuracy of the proposed WDCMM scheme for wheeled mobile manipulators.

Note that we conduct the simulations with different values of ν and η, but, due to space limitations, some results are omitted here. In summary of the simulations, synthesized by the proposed WDCMM scheme, the manipulability of the WMSDM is increased, and the manipulator system is kept away from singularities. In addition, the WDCMM scheme has the ability to remedy the joint variables' abrupt change problem. These results demonstrate well the efficacy, accuracy and superiority of the proposed WDCMM scheme.

V. Conclusion

This paper has designed, proposed and studied the novel weighted damping coefficient based manipulability maximizing (WDCMM) scheme (4) for the optimal control of mobile robot manipulators. Then, the wheeled mobile manipulator composed of the six-DOF spatial manipulator and the wheeled mobile platform has been introduced. Moreover, in order to verify the efficacy and superiority of the proposed WDCMM scheme, comparative simulations based on the presented wheeled mobile manipulator have been carried out, with two end-effector path-tracking examples given. Simulation results have further demonstrated the proposed WDCMM scheme's ability to remedy the MDJVA problem as well as its efficacy, superiority and accuracy on the motion planning of wheeled mobile manipulators. Note that the proposed WDCMM scheme is investigated at the velocity level, and we expect to generalize the scheme at higher levels (e.g., acceleration level or torque level) for the motion planning of mobile robot manipulators in the future work.

References

[1] Y. Zhang, J. Li, and Z. Zhang, "A time-varying coefficient-based manipulability-maximizing scheme for motion control of redundant robots subject to varying joint-velocity limits," Optim. Control Appl. Meth., vol. 34, no. 2, pp. 202–215, 2013.

[2] B. Siciliano and O. Khatib, Springer Handbook of Robotics, Heidelberg: Springer, 2008.

[3] K. Nagatani, T. Hirayama, A. Gofuku, and Y. Tanaka, "Motion planning for mobile manipulator with keeping manipulability," Proc. IEEE Int. Conf. Intell. Robots Syst., pp. 1663–1668, 2002.

[4] J. Baillieul, J. M. Hollerbach, and R. W. Brockett, "Programming and control of kinematically redundant manipulators," Proc. 23rd IEEE Conf. Decision Control, pp. 768–774, 1984.

[5] B. Bayle, J. Y. Fourquet, and M. Renaud, "Manipulability of wheeled mobile manipulators: application to motion generation," Int. J. Robot. Res., vol. 22, no. 7–8, pp. 565–581, 2003.

[6] L. Xiao and Y. Zhang, "A new performance index for the repetitive motion of mobile manipulators," IEEE Trans. Cybern., vol. 44, no. 2, pp. 280–292, 2014.